

Document downloaded from:

[\[http://redivia.gva.es/handle/20.500.11939/6203\]](http://redivia.gva.es/handle/20.500.11939/6203)

This paper must be cited as:

[Cubero, S.; Albert, F.; Manuel Prats-Moltalban, J.; Fernandez-Pacheco, D. G.; Blasco, J.; Aleixos, N. (2018). Application for the estimation of the standard citrus colour index (CCI) using image processing in mobile devices. *Biosystems Engineering*, 167, 63-74.]

**ivia**  
Institut Valencià  
d'Investigacions Agràries

The final publication is available at

[\[https://doi.org/10.1016/j.biosystemseng.2017.12.012\]](https://doi.org/10.1016/j.biosystemseng.2017.12.012)

Copyright [Elsevier]

# Application for the estimation of the standard Citrus Colour Index (CCI) using image processing in mobile devices

S. Cubero<sup>1</sup>, F. Albert<sup>2</sup>, J.M. Prats-Moltalban<sup>3</sup>, D.G. Fernández-Pacheco<sup>4</sup>, J. Blasco<sup>1</sup>, N. Aleixos<sup>2\*</sup>

<sup>1</sup>Centro de Agroingeniería. Instituto Valenciano de Investigaciones Agrarias (IVIA). CV-315, km 10,7 – 46113 Moncada (Valencia), Spain

<sup>2</sup>Departamento de Ingeniería Gráfica, Universitat Politècnica de València, Camino de Vera s/n, 46022 Valencia, Spain. Email: naleixos@dig.upv.es

<sup>3</sup>Grupo de Ingeniería Estadística Multivariante, Departamento de Estadística e IO Aplicadas y Calidad, Universitat Politècnica de València, Camino de Vera s/n, 46022 Valencia, Spain

<sup>4</sup>Departamento de Expresión Gráfica, Universidad Politécnica de Cartagena, Cartagena 30202, Spain

**Abstract** The collection of oranges normally begins before they have reached the typical orange colour. Moreover, citrus fruits are subjected to certain degreening treatments that depend on the standard citrus colour index (CCI) at harvest. In order to facilitate the measure of this index, a free application that uses image processing techniques has been developed for Android-based mobile devices using the built-in camera of the device. The image analysis process is performed on all the images from the live input of the camera to obtain the CCI of such fruit using the open source OpenCV library. For this purpose, the RGB (red, green and blue colour coordinates) average value of a pre-selected area of the input image is calculated and then converted to HunterLab colour space to finally calculate the CCI. Several tests were carried out in the field with the fruit in the trees and under laboratory conditions with different varieties of oranges (Navel, Bonanza, Cram and Navelina) at different stages of maturity, and using different Android devices. The results were obtained for each device and condition in relation to the colour measured by a camera and compared with the performance of a panel of workers who evaluated the colour using the traditional methods. Best  $R^2$  values obtained were 0.854 for outdoors conditions and 0.881 when measurements were done indoors.

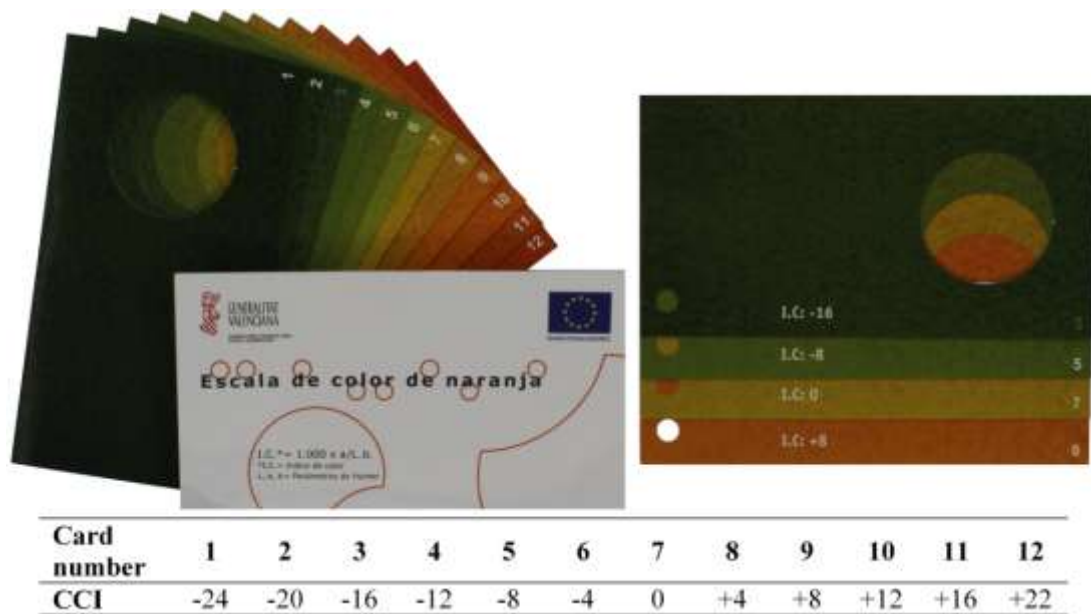
**Keywords:** mobile device, colour analysis, citrus fruits, Colour Citrus Index estimation, in-field conditions

## 1. Introduction. State of the art

Colour is one of the main attributes that consumers associate directly with the freshness or maturity of agricultural food products, so it is a key factor in their preferences over other

36 products (Campbell et al., 2004). A practical application where the inspection of the colour is  
37 also needed is the marketing of citrus fruits. Fruits are harvested manually, loaded in boxes  
38 and transported to packing houses, where they are sorted in batches. In the early season,  
39 when the citrus fruit is received in the packinghouse, this sorting focuses on classifying by  
40 colour because it normally needs a degreening treatment using ethylene, whose duration  
41 depends on the colour they present at harvest (Porat, 2008). The standard parameter used to  
42 determine the colour of citrus fruits is the citrus colour index (CCI), being used in the citrus  
43 industry to determine the harvesting date and to decide which fruit should undergo a  
44 degreening treatment and the type of the treatment (Jimenez-Cuesta et al., 1981).

45 The common way to determine the CCI in the industry is by using colorimeters, which are  
46 specific electronic devices for colour measurement that express colours as numerical  
47 coordinates. However, although colorimeters give accurate colour measures and are small  
48 handy devices, they are expensive and only provide information of a very small area of the  
49 fruit surface (Gardner, 2007), which may not be representative of the colour information of  
50 the whole fruit surface, especially when the fruit has not a uniform colour. In this sense,  
51 calibrated colour cameras can achieve similar results to colorimeters (Vidal et al., 2013).  
52 Another extended way to estimate the CCI is the set of cards simulating the colour and  
53 texture of the fruit at different stages of maturity developed by the Centro de Tecnología  
54 Postcosecha of the Instituto Valenciano de Investigaciones Agrarias (IVIA) and provided by  
55 the Consellería de Agricultura Pesca y Alimentación of the Generalitat Valenciana for  
56 oranges (Fig. 1) and mandarins, which allows a visual comparison of the citrus surface to the  
57 printed colour inside a circular window and so estimate the CCI of such fruit that is printed  
58 on each colour card (DOGV, 2006).



59

60 **Figure 1.** Set of coloured texture cards used to estimate visually the CCI of oranges

61

62 A way to automate this measurement is to acquire images of the fruit using digital cameras  
 63 and then analysing the colour using image processing software. This method allows  
 64 estimating the colour of a bigger region or even the entire fruit, being especially suitable in  
 65 those cases where the surface has a heterogeneous colour since the colours of the pixels are  
 66 determined individually (Cubero et al., 2011; Lorente et al., 2012). Automated estimation of  
 67 colour using image processing presents several advantages regarding the visual inspection  
 68 such as accuracy, objectivity and repeatability. However, one of the major drawbacks when  
 69 measuring colour using images is that, normally, the colour is provided in red, green and  
 70 blue colour coordinates (RGB) since this is the native colour space for most image  
 71 acquisition devices. However, this colour space is device-dependent, and it is not a  
 72 perceptual colour model. On the contrary, other colour models like CIELAB or HunterLab  
 73 are defined in such a way that the distances among colours in the colour space are related  
 74 with the differences in the human perception regardless of the position of the colours, so they  
 75 are very well suited for colour comparison and appropriate for measuring or representing the  
 76 colour of fruits (Mendoza et al., 2006; Arzate-Vázquez et al., 2011; Lang and Hübert, 2012).

77 In most cases, it is necessary to obtain comparable measurements of the colour by using  
 78 colour indices, which combine the colour coordinates in one single ratio easier to be  
 79 understood and handled by operators (Quevedo et al., 2013; Cavazza et al., 2013; Cárdenas-  
 80 Pérez, et al., 2017). The CCI is estimated using a ratio whose definition is based on

81 HunterLab colour coordinates and the colour of application ranges from green to orange.  
82 This index determines the need of degreening treatments and the commercial maturity stage,  
83 two important issues, that differ and depend on the variety (Lado et al., 2014).

84 However, a common vision system needs an external acquisition device (the camera) and the  
85 image processing software, that is normally implemented to be run on a computer, which  
86 prevents to obtain the data instantaneously or to be used in the field, and it is clearly less  
87 practical than the traditional portable texture set of cards or colorimeters. An alternative is  
88 the implementation of the computer vision system in a mobile device like a smartphone.  
89 Currently, a smartphone is a relatively inexpensive hand-held computer with very high  
90 processing capability. In addition, the integration of built-in high resolution sensors and  
91 cameras in these devices makes them practical solutions for many tasks in agriculture and  
92 farming. For example, research has been recently conducted on mobile devices to calculate  
93 solar radiation parameters (Molina-Martínez et al., 2011), real-time livestock monitoring  
94 (Hwang et al., 2013) or prediction of oil palm content (Pamornnak et al., 2015).

95 The capability to acquire and process images allows these devices to be used to obtain  
96 objective and accurate information on the tasks that have traditionally been based on the  
97 experience of trained workers. For instance, Intaravanne et al. (2012) used the built-in  
98 camera of a smartphone to capture images of bananas and estimate their ripeness depending  
99 on the measurement of the colour. In the work developed by Gómez-Robledo et al. (2013), it  
100 is presented an application to evaluate the soil colour implementing a Munsell soil-colour  
101 model. This application used the built-in camera inside a controlled lighting chamber to  
102 capture and store the images that are later processed. Gong et al. (2013) presented an  
103 android-based application with the aim of predicting the yield of citrus orchards by first  
104 acquiring and storing the images and later processing them. The colour information captured  
105 by mobile devices was used to study the structure of coffee branches and determine the  
106 number of fruits by Ramos et al., (2017) and Avendano et al., (2017).

107 A summary of the works that use smartphone-based sensors in agriculture is presented by  
108 Pongnumkul et al. (2015). In this review they report that works that use the built-in  
109 smartphone cameras take pictures or videos which are later sent and stored as a whole on  
110 servers or on the cloud for future reference or further inspection sending back the results to  
111 the mobile-phone, or take pictures or videos to be image-processed further in the very  
112 device. They also state that it is necessary to endow these applications with highly intuitive  
113 interfaces, concluding that many applications still do not concern this aspect.

114 As we can see from the works mentioned above, the user needs to capture and to store the  
115 images first, and then has to start the app developed to analyse them (in the smartphone or in  
116 an external server), since the apps do not work with the live input of the camera, that is, do  
117 not work on-line. The approach presented in here offers a simple and intuitive user interface  
118 and provides a portable, handy and economical innovation for the estimation of the CCI,  
119 working as a real on-line vision system, providing real-time results and allowing the user  
120 avoiding the management of the stored images since the analysis has been performed on the  
121 live camera input.

122 It has been tested using different configurations of the camera and under different  
123 environmental conditions, especially outdoors where the image processing is always more  
124 complex due the changing lighting conditions (Sabzi et al., 2017; Sengupta and Lee, 2014).  
125 The results were obtained for each device and condition in relation to the colour measured by  
126 a calibrated image acquisition system and compared with the performance of a panel of  
127 workers who evaluated the colour using the traditional methods, in order to determine  
128 whether this kind of devices can be potentially accurately used when working both in a  
129 packinghouse or outdoors under natural conditions, thus being a helpful tool to the grower  
130 for crop and commercialisation management.

131

## 132 **2. Materials and Methods**

133 The algorithms of colour estimation have been implemented for Android mobile devices  
134 using the open-source BSD-licensed library OpenCV  
135 ([https://en.wikipedia.org/wiki/BSD\\_licenses](https://en.wikipedia.org/wiki/BSD_licenses)), the open software development kit (SDK) for  
136 Android (<http://developer.android.com/sdk/terms.html>), and the programming environment  
137 Eclipse (<http://www.eclipse.org/org/documents/epl-v10.php>) using Java language. Android  
138 is the most widespread operating system for mobile devices (Puder and Antebi, 2013) and  
139 permits to use and program open-code using a free license. Two sets of devices were used,  
140 the first one (Table 1) was composed of four devices (2 phones and 2 tablets) that were used  
141 to carry out the preliminary tests of the app during the development in the season 2014/15,  
142 and the second set was composed of seven smartphones with different hardware  
143 characteristics (Table 2) and was used to for the final test and validation of the app in real  
144 operating conditions during the next season (2015/16).

145

146 **Table 1.** Devices used to develop and calibrate the app

Device type	Tablet	Tablet	Smartphone	Smartphone
<b>Model</b>	Samsung Tab 2 (GT-P5110)	Ampe A78 Dual Core	Samsung S III (GT-I9300)	Samsung S III Mini (GT-I8190)
<b>Android version</b>	4.0.3	4.2.2	4.1.2	4.1.2
<b>Display</b>	10.1"	7"	4.8"	4"
<b>Resolution display</b>	1280 x 800	1024 x 600	720 x 1280	480 x 800
<b>Built-in camera</b>	3 MP	2 MP	CMOS 8 MP	CMOS 5 MP
<b>CPU*</b>	ARM Cortex-A (2 x 1 Ghz)	RK3066 (2 x 1.6 Ghz)	ARM Cortex-A9 MPcore (4 x 1.4 Ghz)	ARM Cortex-A9 (2 x 1 Ghz)
<b>GPU**</b>	PowerVR SGX540	ARM Mali-400 MP	ARM Mali-400	ARM Mali-400

147 \*Central Processing Unit

148 \*\*Graphics Processing Unit

149

150 **Table 2.** Smartphones used to validate the app

Device number	1	2	3	4	5	6	7
<b>Model</b>	BQ Aquaris M5	Cubot S200	LG Optimus L4 (Tri E470)	LG Nexus 5	Samsung S3	Samsung S3 Mini (GT-I8190)	Sony Xperia P
<b>Android version</b>	5.1.1	4.2.2	4.1.2	6.0.1	4.3	4.1.2	4.1.2
<b>Display</b>	5"	5"	3,8"	5"	4,8"	4"	4"
<b>Resolution display</b>	1080x1920	720 x 1280	320 x 480	1080x1920	720 x 1280	480 x 800	540 x 960
<b>Built-in camera</b>	CMOS 13 MP	CMOS 12.78 MP	CMOS 3.15 MP	CMOS 8 MP	CMOS 8 MP	CMOS 5 MP	CMOS 8 MP
<b>CPU*</b>	Snapdragon 615 Octa Core (8 x 1.5 Ghz)	ARM Cortex-A7 (4 x 1.3 Ghz)	ARM Cortex-A9 (1 x 1 Ghz)	Snapdragon 800 Quad Core (4 x 2.3 Ghz)	ARM Cortex-A9 Mpcore (4 x 1.4 Ghz)	ARM Cortex-A9 (2 x 1 Ghz)	ARM Cortex-A9 (2 x 1 Ghz)
<b>GPU**</b>	Adreno 405 550 MHz	ARM Mali-400 500 MHz	PowerVR SGX531	Adreno 330 550 MHz	ARM Mali-400 500 MHz	ARM Mali-400 500 MHz	ARM Mali-400 500 MHz

151 \*Central Processing Unit

152 \*\*Graphics Processing Unit

153

### 154 3. Description of the application

155 The interface is developed to facilitate the operation of colour measurement by the grower.

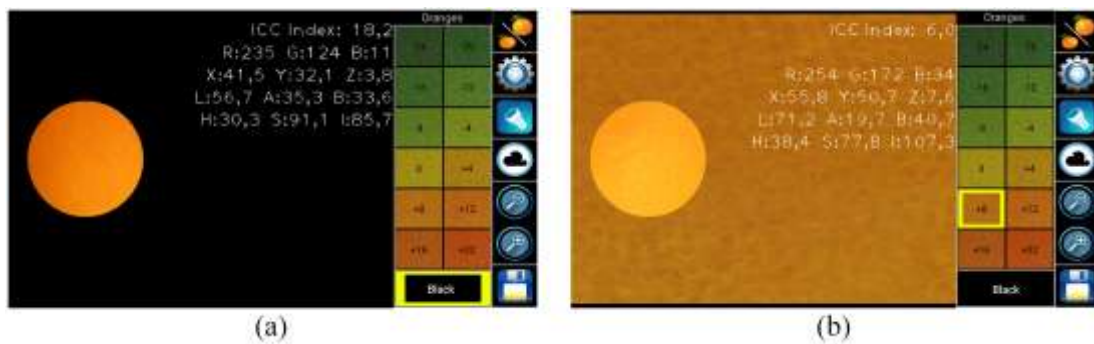
156 When the application runs, the device display is configured in landscape mode with two

157 well-differentiated zones: the left part being to capture the images and display the results;

158 and the right area of the screen to configure the app (Fig. 2). To facilitate the colour

159 measurement in all conditions, the app can operate in two modes, by comparison with a  
160 colour reference card or of colour estimation by real-time image processing.

161 The first method contains the preview of the standard coloured texture cards (Fig. 1) for  
162 visual comparison with the sample. Two sets of cards can be selected for oranges and  
163 mandarins. When it is active, the texture card corresponding to the selected texture preview  
164 is superimposed to the image zone and the obtained CCI is given by the indicative value of  
165 the card (Fig. 2b). This method simply substitutes the current physical colour cards by virtual  
166 cards thus facilitating the opportunity of taking measurements with the advantage of  
167 recording the results. However, as the number of cards is limited, the method presents  
168 limitations and the colour of the sample must be approached to the most similar card, which  
169 has a lack of accuracy. Alternatively, in the second method, the app estimates the colour of  
170 the sample in real-time presenting the measurement of the colour using the CCI and also  
171 different colour coordinates (if selected).



172 (a)  
173 **Figure 2.** Interface of the application: (a) Information from image analysis is available; and  
174 (b) Set of coloured textures active for alternative visual comparison

175  
176 The camera is the key device feature in this application but, depending on the model, the  
177 characteristics of the optics, the sensor, and their configuration and performance can vary.  
178 An important feature to properly measure the colour is the white balance (WB) that is the  
179 process of removing unrealistic colour casts, so that objects which appear white to the human  
180 eye are rendered white in the photo. Proper camera WB has to take into account the colour  
181 temperature of the light source. By default, the auto mode for the WB is set. However,  
182 depending of the illumination of the scene it is possible to choose other particular WB modes  
183 to obtain accurate CCI measurements. In addition, the lantern can be turned on to capture the  
184 images if necessary. Other settings allow setting the size of the measuring spot or the  
185 estimated colour information of the fruit in real-time that will be displayed in the screen  
186 while capturing the images.



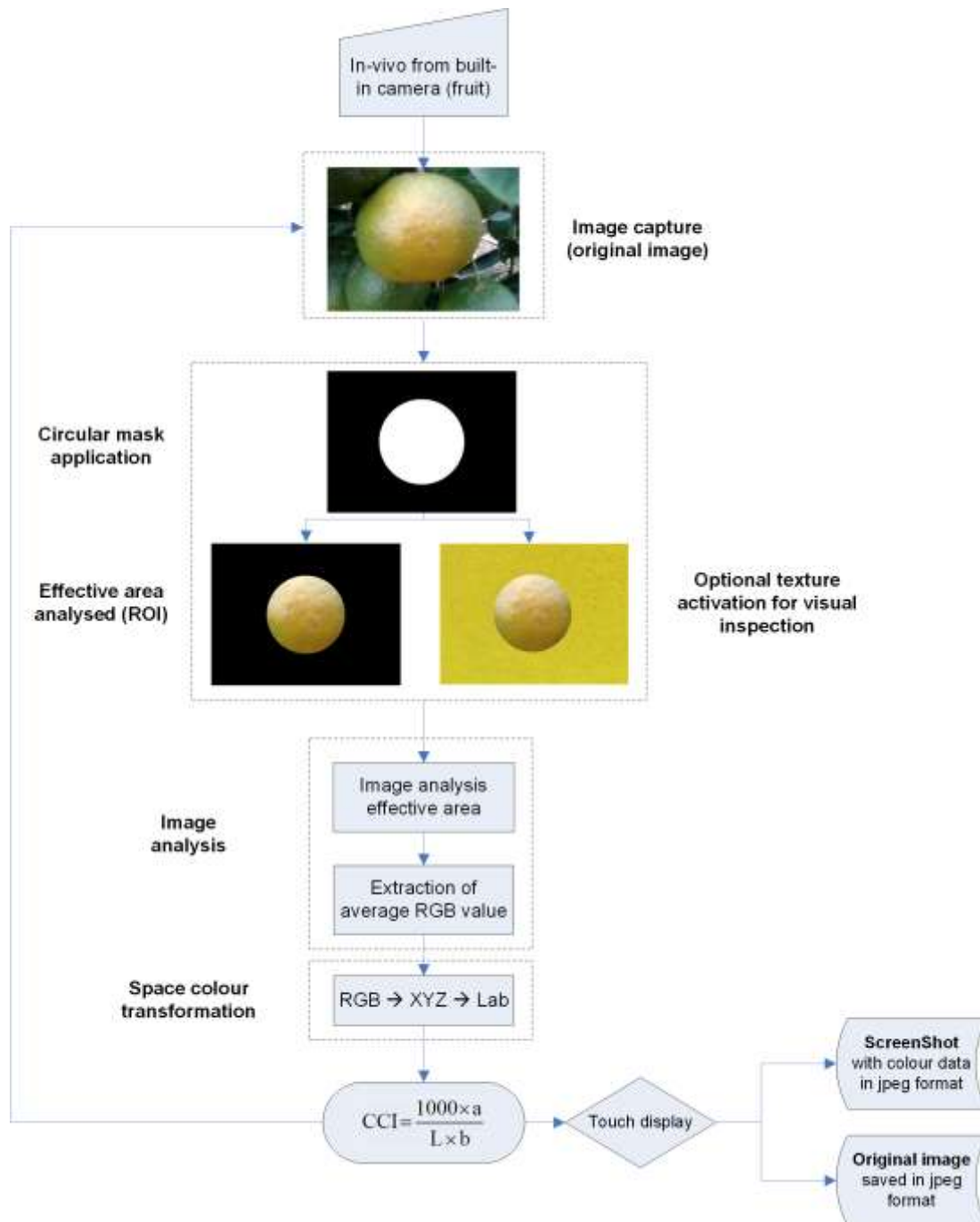
187 The application shows a circular mask area as region of interest (ROI) in which the colour  
188 data is measured and is located close to the built-in camera position at most devices. Thus, in  
189 the case the lantern is activated, the captured scene is properly illuminated. The circular ROI  
190 can be enlarged or reduced as desired to obtain accurate measurements depending on the  
191 distance to the sample or if the application is used in the field or indoors. If illumination is  
192 good, a bigger area can be measured.

193 Once the application is running, the camera shows the live image inside the ROI, and  
194 presents the colour information from the sample in real-time. The process to obtain the CCI  
195 in real-time begins with the calculation of the average RGB value from all the pixels of the  
196 ROI. Then, this value is converted to XYZ colour coordinates using equations described by  
197 Mendoza et al. (2006), and finally XYZ are converted into Hunter Lab values using the  
198 equations corresponding to the illuminant D65 and observer 10° described in HunterLab  
199 (1996). Once this conversion is performed, the CCI is calculated using equation (1), where  $L$ ,  
200  $a$ ,  $b$  are the coordinates of the Hunter Lab colour space:

$$CCI = \frac{1000 \times a}{L \times b} \quad (1)$$

201 The CCI could probably be more accurately calculated by averaging the CCI value of each  
202 individual pixel but the conversion process for each pixel is time consuming for a real-time  
203 process and the results were proved virtually to be the same by Cubero et al. (2014) and  
204 Vidal et al. (2013). Apart from the colour index, colour information of the ROI in different  
205 colour spaces is also given if they are selected from the preferences menu. The colour spaces  
206 provided are RGB, XYZ, CIELAB and HIS (hue, intensity and saturation coordinates). In  
207 addition, the information about CCI and other colour spaces can be saved along with the  
208 image of the fruit and a screenshot of the device showing all data and configuration. Figure 3  
209 shows the flowchart of the vision-based algorithm of the application developed.

210



211

212 **Figure 3.** Flowchart of the vision-based algorithm of the mobile application developed

213

#### 214 4. Development and calibration

##### 215 4.1 Fruit used in the experiments

216 A total of 55 oranges of different varieties (Navel, Bonanza, Cram and Navelina) at different

217 stages of maturity were used for the tests. Fruits were chosen between November 2014 and

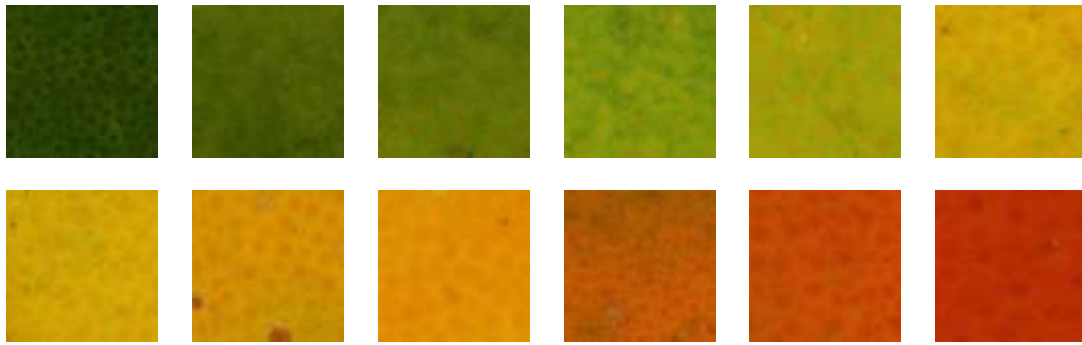
218 March 2015 from experimental parcels at IVIA. The colour of the selected fruits ranged from  
219 uniform dark green to uniform orange including yellowish green to greenish orange to cover  
220 most of the possibilities that can be found in the field. All measurements were carried out in  
221 different sunny days between 11:00 AM and 01:00 PM. Each fruit was labelled and the  
222 colour was measured with the four mobile devices under both field conditions (in the tree  
223 before harvest) and indoor conditions (collected fruits).

224

225 To obtain the reference colour of each fruit, all oranges were photographed using a digital  
226 single lens reflex (DLSR) camera (EOS 550D, Canon Inc, Japan) used to acquire high  
227 quality images with a size of 3456 x 2304 pixels and a resolution of 0.03 mm/pixel. This  
228 reference images were taken by placing each sample inside an inspection chamber  
229 containing the camera and the lighting system. The camera was placed at a distance of 20 cm  
230 from the samples. Illumination was achieved using four lamps that contained two fluorescent  
231 tubes each (Biolux L18W/965, 6500 K, Osram AG, Germany). The angle between the axis  
232 of the lens and the sources of illumination was of approximately 45° since the diffuse  
233 reflection responsible for the colour occurs at 45° from the incident light. However, the  
234 samples have a curved shape that can still produce bright spots affecting the colour  
235 measurements. In order to minimise the impact of these specular reflections, cross  
236 polarisation was used by placing polarising filters in front of the lamps and in the camera  
237 lenses. The fluorescent tubes were powered using high frequency electronic ballast to avoid  
238 the flickering effect of the alternate current and produce a more stable light. The application  
239 EOS utility (Canon Inc, Japan) was used to capture the images of each fruit. This software  
240 allows tuning all the camera parameters like the ISO, shutter speed or resolution as well as  
241 capturing the images without handling the camera. A colour calibration was performed to the  
242 images obtained with this camera using a standardised colour chart (ColorChecker SG Chart,  
243 X-Rite Inc, USA). The colours of the patches in the colour chart were correlated with those  
244 provided by the maker achieving a determination coefficient  $R^2$  higher than 99.9 %.

245 In addition, a semi-trained panel composed of nine experts measured later the colour of the  
246 fruits visually using the standard colour cards. Figure 4 shows representative samples of the  
247 colour of the fruit used in all the experiments.

248



249 **Figure 4.** Representative samples of the colour of the fruit used for the experiments

250

#### 251 4.2 Description of the tests

252 In order to achieve the previous stated objectives, several tests were carried out:

- 253 1. The CCI of each fruit was measured using all four mobile devices in the field, with the  
254 fruits in the trees before harvesting (Fig. 5a). This is important to know the performance  
255 of the application when working in field conditions to be used as a tool to aid in the  
256 decision of the harvesting moment. The CCI was estimated using different WB modes  
257 such as auto, cloudy, fluorescent, and with the flash activated.
- 258 2. Later, each fruit was harvested and labelled and its CCI was measured in the laboratory  
259 with all four mobile devices under controlled illumination using the same WB options  
260 than in the field (Fig. 5b).
- 261 3. The colour of all fruits was later measured using the reference DLSR camera. Four  
262 measurements were acquired; two in the equatorial part, one near the stem-end and  
263 another near the blossom-end. The RGB colour coordinates of the fruit were converted  
264 to Hunter Lab values following the same algorithm developed for the app.
- 265 4. Finally, the CCI of each fruit was estimated by the semi-trained panel of nine workers  
266 (inspectors) who annotated their judgement using the traditional current standard texture  
267 colour cards.

268

269



270

271

(a)

(b)

272 **Figure 5.** Different test conditions: (a) under field conditions; and (b) under controlled  
 273 illumination conditions

274

275 Then, for each fruit, the CCI was measured with the mobile devices under field conditions  
 276 and under laboratory conditions with three different white balance modes, using the DLSR  
 277 camera and by the semi-trained panel. The CCI values calculated by using the mobile  
 278 devices in different conditions were compared to those obtained using the reference and the  
 279 panel. The statistical analysis of data was performed through multiple regression models  
 280 (Montgomery, 2005) using Statgraphics Centurion (StatPoint Technologies, USA) statistical  
 281 software. Results achieved during development were used to improve the application and  
 282 perform the validations tests.

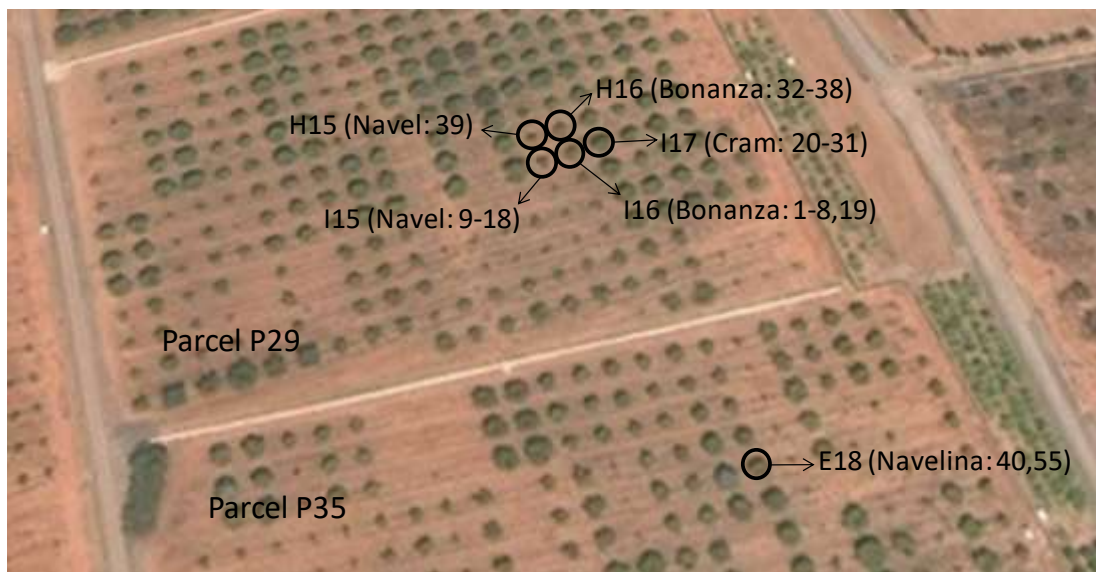
283

## 284 5. Validation

285 Both, the images captured during development and the results obtained allowed  
 286 incorporating a number of improvements to make the app more robust and the colour  
 287 measurement more accurate under different conditions. To validate the app, the tests  
 288 performed for development were repeated in the field and laboratory in the next season  
 289 between November 2015 and March 2016 to cover all colour range during the natural  
 290 maturation process of the fruit. The experiments were the same than those performed for the  
 291 calibration but using all devices listed in the Table 3. The colour of 230 different oranges  
 292 was measured with each device in the same trees in the field in different days between 11:00  
 293 AM and 01:00 PM under sunny conditions, and indoor simulating the illumination of a  
 294 packinghouse. In the test performed to calibrate the app, all the images were captured using

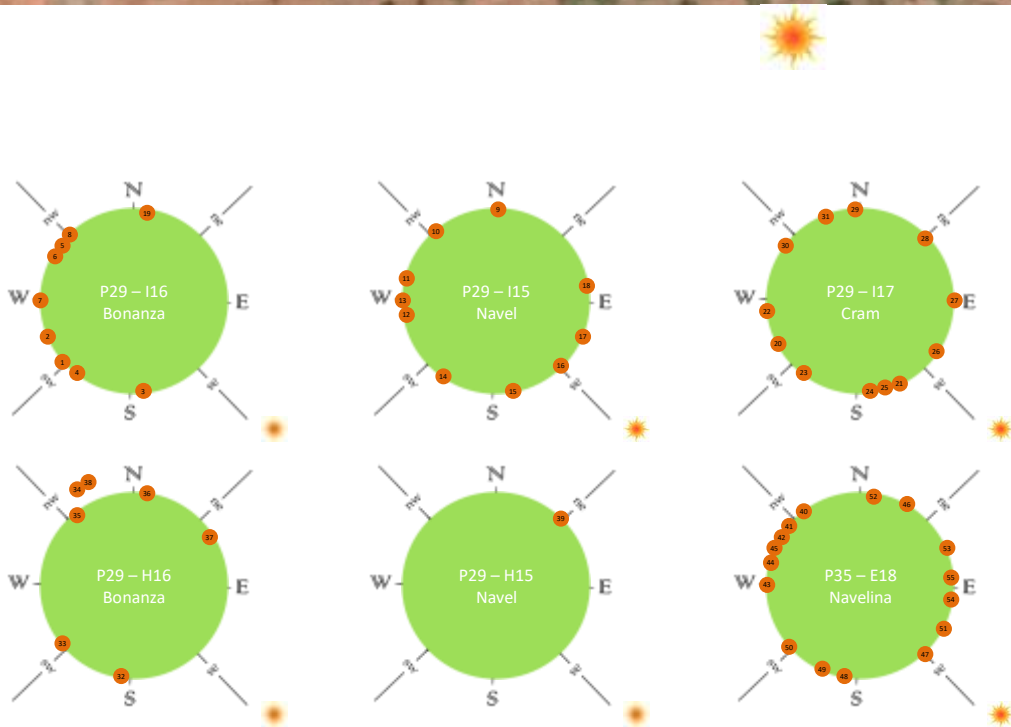
295 automatic WB, but to validate the application, the images were captured using different WB  
 296 modes like AUTO, CLOUDY, FLUORESCENT, and with the FLASH activated. Figure 6  
 297 shows the trees selected from the experimental parcels at the IVIA (top image) and the  
 298 relative position of the fruits in the trees with the position and orientation of each tree  
 299 regarding the location of the sun (bottom image) in order to cover different conditions  
 300 regarding the sun location.

301



302

303



304

305 **Figure 6.** Top image: trees surveyed at the experimental parcels at the IVIA including the  
 306 position of the sun; and bottom image: location and relative orientation of the fruits in the  
 307 trees

308

309 **6. Results and discussion**

310 6.1 Performance under different conditions with all the devices

311 One way for assessing the reliability of the method proposed when working with different  
 312 cameras and under different conditions is to compare the value of the coefficient of  
 313 determination  $R^2$  of the Multiple Regression models between each of the tested built-in  
 314 cameras (smartphones) and the reference DLSR camera. This coefficient provides the ratio  
 315 between the models explained variability and the total variability of the data, *i.e.* the  
 316 proportion (percentage) of the CCI values that can be predicted by the model. This is  
 317 achieved by computing different regression models, using the CCI values of the reference  
 318 camera as dependent variables, and the CCI values of the different smartphones as  
 319 independent variables. In all cases, linear and non-linear terms (up to fourth polynomial)  
 320 were included in the models, using one or the other depending on the statistical significance  
 321 (for a Type I risk of 0.05) of the coefficients, in a backward elimination sequential  
 322 procedure. The  $R^2$  values for the different devices analysed are presented in Table 3, for each  
 323 device and WB mode tested, and for each of the two conditions (outdoors and indoors). The  
 324 results achieved by the FLORESCENT WB mode are not presented because in all cases the  
 325 results achieved were poor. In order to assess for statistical significant differences between  
 326 devices, environmental conditions and white balance modes, analysis of variance (ANOVA)  
 327 was carried out on these  $R^2$  values. Table 4 shows the results of the corresponding analysis.

328 **Table 3.**  $R^2$  values achieved for the different built-in cameras analysed under outdoors and  
 329 indoors conditions

Device	Outdoors			Indoors		
	AUTO	FLASH	CLOUDY	AUTO	FLASH	CLOUDY
1	0.796	0.854	0.739	0.813	0.831	0.791
2	0.715	0.737	0.585	0.876	0.842	0.728
3	0.684	0.703	0.721	0.881	0.838	0.872
4	0.725	0.795	0.679	0.818	0.834	0.844
5	0.737	0.798	0.232	0.830	0.820	0.401
6	0.708	0.766	0.278	0.774	0.753	0.484

7            0.723            0.698            0.697            0.806            0.743            0.715

330  
331  
332

**Table 4.** ANOVA of the  $R^2$  values achieved for the different built-in cameras analysed

Source	Sum of Squares	Df*	Mean Square	F-ratio	P-value
<b>Main effects</b>					
A: Device	1845.520	6	307.586	28.65	0.0000
B: Environment	880.551	1	880.551	82.01	0.0000
C: WB mode	2272.650	2	1136.330	105.83	0.0000
<b>Interactions</b>					
AB	218.408	6	36.401	3.39	0.0341
AC	3001.250	12	250.105	23.29	0.0000
BC	131.895	2	65.947	6.14	0.0146
Residuals	128.843	12	10.737		
Total (corrected)	8479.120	41			

333 \*Degrees of freedom

334 From these results, the most relevant findings are that when the app is used indoors  $R^2$  values  
335 are higher and it performs better than in the field, which is quite expected since the  
336 illumination conditions are more stable for the former condition. However, interaction  
337 effects appear between the device, the environments and the white balance mode, which  
338 means that they are interconnected, and that different conclusions can be drawn depending  
339 on, i.e., the environment where the pictures are obtained.

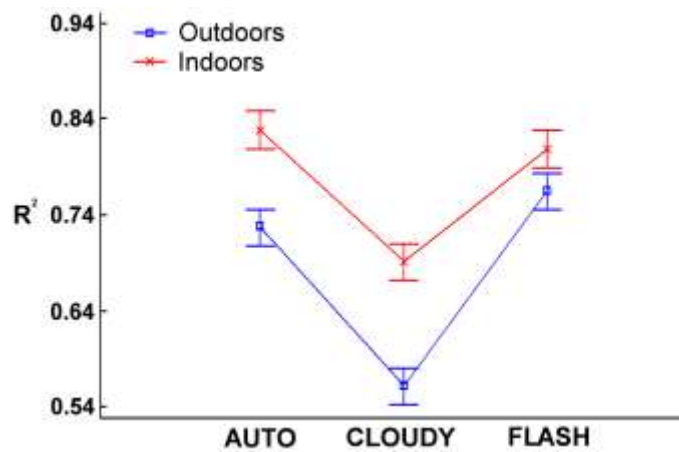
340 Figures 7 and 8 show the different interaction plots, which are afterwards analysed to derive  
341 the most relevant achievements. From these figures, it can be seen (Fig. 7) that, although the  
342 measurements taken under indoors environment present higher  $R^2$  values, these differences  
343 are reduced when working with the flash activated. Actually, within the outdoors conditions,  
344 it can be seen that mode FLASH presents statistically significant differences with mode  
345 AUTO, probably because this way, the colours are homogenised, the light directly coming  
346 from the sun is attenuated and the shadows are cleared. On the contrary, in the indoor  
347 conditions these differences cannot be stated. Finally, CLOUDY mode obtained poorer  
348 results, especially in the field, which can be explained by the existing sun conditions when  
349 the images were taken. It should be noted that CLOUDY mode was selected because, under



350 indoor conditions, it seemed to be better visually matching the colors of oranges than with  
351 other modes, which in the light of the results obtained was clearly incorrect.

352 Analysing each device independently, from Table 3, it can be seen that device 1 (BQ Aquaris  
353 M5) shows the best results when working in the field, especially when the flash is activated,  
354 equivalent to those obtained under well-controlled indoors conditions. When the fruit was  
355 inspected under conditions similar to those found in a commercial packinghouse, the results  
356 were better, performing best the device 3 (LG Optimus L4). However, no large differences  
357 were found among the first four devices. In this case, the best results were achieved using the  
358 auto WB, except in some cases so the recommendation is to set this mode on. Comparison  
359 between conditions and devices can be seen in the interaction plots shown in Figures 7 and 8.

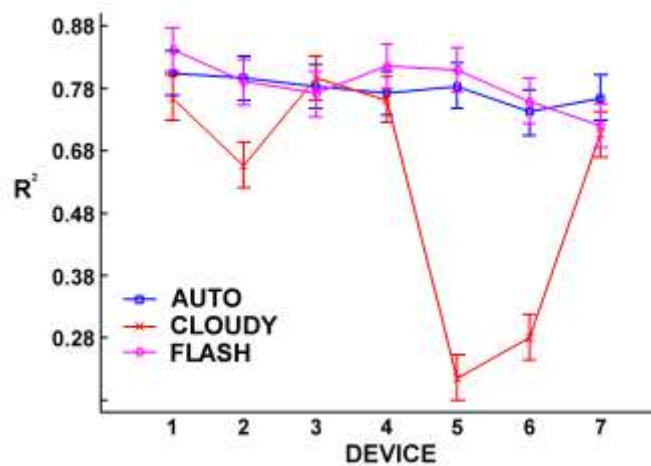
360



361

362 **Figure 7.** Interaction plot for the WB mode and the two environmental conditions

363



364

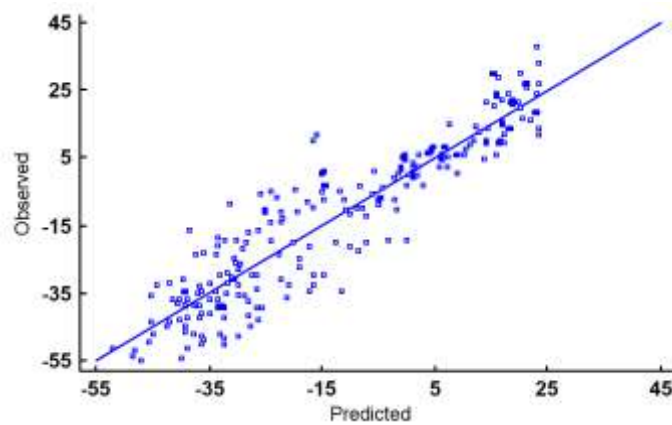
365

**Figure 8.** Interaction plot for the Device and WB mode

366

367 Summarising, when the app is used in the field to estimate the colour of the oranges in the  
368 trees, device 1 shows the best performance. Actually, no statistical significant differences  
369 appear between the different modes used although for illustration purposes the mode with the  
370 flash activated is depicted in Figures 9 and 10, showing the relation between the values  
371 predicted with the device and the reference camera, both in the field (Fig. 9) and indoors  
372 (Fig. 10).

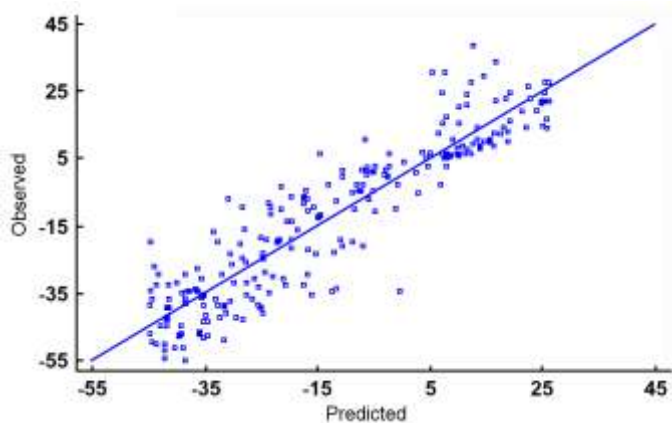
373



374

375 **Figure 9.** Observed vs predicted CCI values for Device 1 and FLASH mode in outdoors  
376 conditions ( $R^2$  value 0.854)

377



378

379 **Figure 10.** Observed vs predicted CCI values for Device 1 and FLASH mode in indoors  
380 conditions ( $R^2$  value 0.831)

381

382 These results give confidence on the ability of the built-in cameras of smartphones to  
 383 reproduce the CCI values obtained with a reference camera, taking into account the huge  
 384 variability and heterogeneity of the colours of the citrus fruits, especially when they are  
 385 turning from green to orange, and when CCI values of the reference camera were obtained  
 386 under well-controlled laboratory conditions.

387 Since FLASH mode shows the most robust results (i.e. the ones with minor statistical  
 388 differences in their means for all devices, no matter if the camera is working outdoors or  
 389 indoors), the following analyses were carried out using this WB mode.

390

## 391 6.2 Comparison to human performance

392 The current method to evaluate the colour of the citrus before or at harvest is based on the  
 393 subjective estimation of workers by comparison with printed colour patterns. In order to  
 394 compare the CCI values estimated by different workers to those computed by the mobile  
 395 devices, the same dataset was also analysed by nine experts. ANOVA was carried out to  
 396 compare the results of all devices ( $R^2$ ) with this new application configured to use the  
 397 FLASH WB mode in both indoors and outdoors conditions.

398

### 399 6.2.1 Comparison of the human performance with all devices in outdoors conditions

400 Table 5 presents the ANOVA table, and Figure 11a the least significant difference (LSD)  
 401 comparison between the devices working outdoors and the human inspection. It can be seen  
 402 how the inspectors provide a better relation with the reference camera, i.e. higher  $R^2$  values,  
 403 with a high statistical significance (very low *p-value*).

404

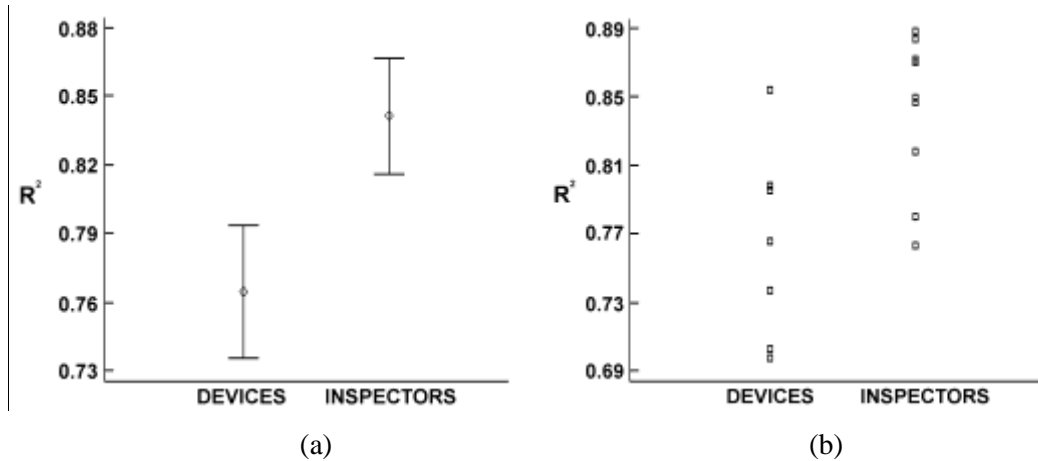
405 **Table 5.** ANOVA table for  $R^2$  values achieved for the two types of judges analysed: Devices  
 406 vs Inspectors, outdoors conditions.

Source	Sum of Squares	Df*	Mean Square	F-ratio	P-value
Judge	231.648	1	231.648	9.12	0.0092
Residuals	355.787	14	25.4134		
Total (Corrected)	587.436	15			

407 \*Degrees of freedom

408 Nevertheless, when inspecting the Scatter plot in Figure 11b, it can also be seen how the  $R^2$   
 409 values from both the devices and the inspectors overlap considerably. Furthermore, the

410 estimation performed by the inspectors was carried out under well illuminated indoors  
 411 conditions, while the image measurements were taken under changing natural conditions  
 412 with the sun illuminating the fruits from different positions, so a fair comparison between  
 413 them would be that in indoors.



414  
 415

416 **Figure 11.** Comparison between the devices working outdoors and the human inspection. (a)  
 417 LSD plot for judge; and (b) Scatter plot for judge (Devices vs. Inspectors)

418

#### 419 6.2.2 Comparison of the human performance with all devices in indoors conditions

420 When repeating the analysis for the indoors conditions, no statistical significant differences  
 421 can be assessed between devices and inspectors, as the p-value in Table 6 is higher than the  
 422 alpha or Type I risk used (5 %), defined as the risk of rejecting the Null hypothesis when in  
 423 fact it is true. This can be also derived from the fact that the two LSD intervals in Fig. 12a  
 424 overlap.

425

426 **Table 6.** ANOVA table for  $R^2$  values achieved for the two types of judges analysed: Devices  
 427 vs Inspectors, for indoors conditions

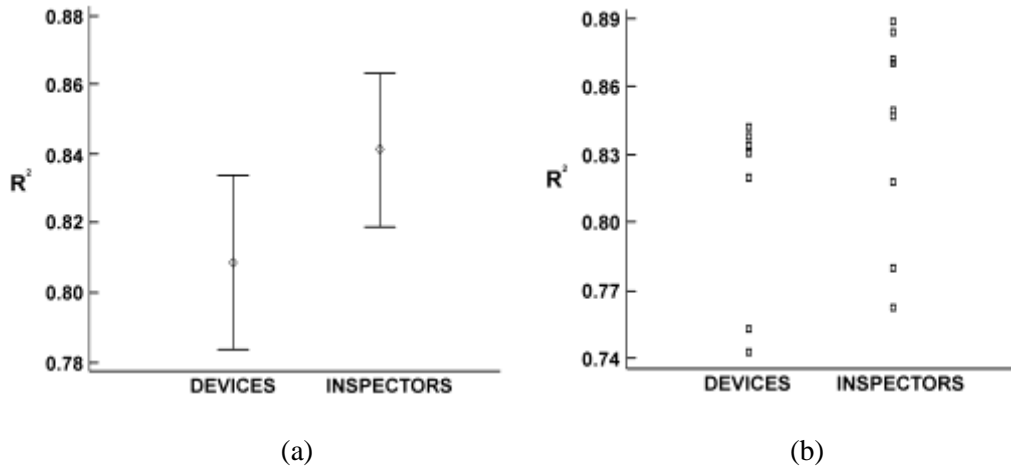
Source	Sum of Squares	Df*	Mean Square	F-ratio	P-value
Judge	41.9971	1	41.9971	2.16	0.1634
Residuals	271.641	14	19.4029		
Total (Corrected)	313.638	15			

428 \*Degrees of freedom

429 Finally, when taking a look at the scatter plot in Fig. 12b, it is possible to see the high degree  
 430 of overlapping between judges, so in the end it is possible to say that, when working in the

431 same conditions, if there is no interaction between judges and environmental conditions  
432 (indoors or outdoors), both types of estimations are equivalent.

433



434

435

436 **Figure 12.** Comparison between the devices working indoors and the human inspection. (a)  
437 LSD plot for judge; and (b) Scatter plot for judge (Devices vs. Inspectors)

438

439 This agricultural app presents certain benefits. It represents a clear advance on the current  
440 visual methods since it introduces objectivity in the colour estimation and substitutes the  
441 current dated colour cards, which are limited to a few number of discrete CCI values  
442 compared to our developed tool capable of obtaining more accurate continuous values. Other  
443 clear advantages are, for instance, the possibility of saving the images for later checking, the  
444 creation of historical reports, the immediate availability for the grower and potential  
445 integration with other tools, and besides its low cost, portability and availability of mobile  
446 technology, being intuitive even for non-specialised personnel. On the other hand, high  
447 amount of possible natural conditions reduces the performance of the app when it is used in  
448 the field, making necessary more research to analyse and discard nonsense colours, bright  
449 spots and discriminate between illuminating conditions to make appropriate colour  
450 corrections that are expected in further versions. In summary, the results are acceptable in  
451 comparison with the method currently used in the industry or by the growers, representing a  
452 clear advance over the current state of the art, since it eliminates the subjectivity but more  
453 research improvements are needed to the image segmentation and CCI estimation reach  
454 human performance.

455

456 **6 Conclusions**

457 A real portable computer vision system that allows measuring the colour index of citrus  
458 fruits automatically, while the fruit is being harvested or under any other process, has been  
459 developed to work with built-in smartphone cameras and successfully tested. The main  
460 advantages are the universal availability of such systems, the portability of this sort of  
461 technology and the simplicity of use of the app, allowing estimating the colour condition of  
462 the fruit (citrus) in the field by means of a real vision system and thus the amount of  
463 degreening processes needed.

464 The system developed has been implemented on the Android operating system and requires a  
465 minimal interaction of the user, providing a live image of the fruit while it is being inspected.  
466 This is a key feature, since no smartphone-based application developed provides this feature,  
467 thus allowing any non-expert user to get use to this application easily.

468 The development of the app was done during one season and it was validated in the next  
469 season with different fruit. Three validations were done, the first and second one to compare  
470 the CCI values from the mobile devices operating under natural (outdoors) and controlled  
471 (indoors) conditions respectively, to those obtained by the reference camera. The  
472 measurements in the field are negatively influenced most probably by the changing  
473 illumination conditions, and this fact lowers the correlation to the reference. The third has  
474 compared CCI values from the mobile devices to those estimated by an expert panel using  
475 the colour cards under the same controlled conditions.  $R^2$  values of 0.854 and 0.881 were  
476 obtained for outdoors and indoors conditions although the results were influenced by the  
477 quality of the mobile device. The obtained results are promising and demonstrate the  
478 feasibility of a smartphone integrated computer vision system to inspect the colour of citrus  
479 fruits in real time in outdoor conditions while the fruit is being harvested, which is a valuable  
480 step forward for this industrial sector.

481

482 **Acknowledgements**

483 This work was partially funded by INIA and FEDER funds through research project  
484 RTA2015-00078-00-00.

485

486 **References**

487 Arzate-Vázquez, I., Chanona-Pérez, J.J., Perea-Flores, M.J., Calderón-Domínguez,  
488 G., Moreno-Armendáriz, M.A., Calvo, H., Godoy-Calderón, S., Quevedo, R., Gutiérrez-  
489 López, G. (2011) Image processing applied to classification of avocado variety Hass (*Persea*  
490 *americana* Mill.) during the ripening process. Food and Bioprocess Technology, 4, 1307-  
491 1313

492 Avendano, J. Ramos, P.J. Prieto, F.A. (2017) A system for classifying vegetative structures  
493 on coffee branches based on videos recorded in the field by a mobile device. Expert Systems  
494 with Applications, 88, 178-192

495 Campbell, B.L., Nelson, R.G., Ebel, C.E., Dozier, W.A., Adrian, J.L., Hockema, B.R. (2004)  
496 Fruit quality characteristics that affect consumer preferences for satsuma mandarins.  
497 HortScience, 39, 1664-1669

498 Cárdenas-Pérez, S., Chanona-Pérez, J., Méndez-Méndez, J.V., Calderón-Domínguez, G.,  
499 López-Santiago, R., Perea-Flores, M.J., Arzate-Vázquez I. (2017) Evaluation of the ripening  
500 stages of apple (Golden Delicious) by means of computer vision system. Biosystems  
501 Engineering, 159, 46-58

502 Cavazza, A., Corradini, C., Rinaldi, M., Salvadeo, P., Borromei, C., Massini, R. (2013)  
503 Evaluation of pasta thermal treatment by determination of carbohydrates, furosine, and color  
504 indices. Food and Bioprocess Technology. 6, 2721-2731

505 Cubero, S., Aleixos, N., Albert, F., Torregrosa, A., Ortiz, C., García-Navarrete, O., Blasco J.  
506 (2014) Optimised computer vision system for automatic pre-grading of citrus fruit in the  
507 field using a mobile platform. Precision Agriculture, 15, 80-94

508 Cubero, S., Aleixos, N., Moltó, E., Gómez-Sanchis, J., Blasco, J. (2011) Advances in  
509 machine vision applications for automatic inspection and quality evaluation of fruits and  
510 vegetables. Food and Bioprocess Technology, 4, 487-504

511 DOGV (2006) Diari Oficial de la Comunitat Valenciana, 5346, 30321-30328

512 Gardner, J.L. (2007) Comparison of calibration methods for tristimulus colorimeters. Journal  
513 of Research of the National Institute of Standards and Technology, 112, 129-138

514 Gómez-Robledo, L., López-Ruiz, N., Melgosa, M., Palma, A.J., Capitán-Vallvey, L.F.,  
515 Sánchez-Marañón, M. (2013) Using the mobile phone as Munsell soil-colour sensor: An  
516 experiment under controlled illumination conditions. Computers and Electronics in  
517 Agriculture, 99, 200–208

518 Gong, A., Yu, J., He, Y., Qiu, Z. (2013) Citrus yield estimation based on images processed  
519 by an Android mobile phone. *Biosystems Engineering*, 115, 162-170

520 HunterLab. 1996. Applications note, Hunter Lab Color Scale.  
521 [https://support.hunterlab.com/hc/en-us/article\\_attachments/201440625/an08\\_96a2.pdf](https://support.hunterlab.com/hc/en-us/article_attachments/201440625/an08_96a2.pdf).  
522 Accessed October 2017.

523 Hwang, J., Jeong, H., Yoe, H. (2013) A study on the real-time livestock monitoring system  
524 using mobile platform. *International Journal of Smart Home*, 7, 137-144.

525 Intaravanne, Y., Sumriddetchkajorn, S., Nukeaw, J. (2012). Cell phone-based two  
526 dimensional spectral analysis for banana ripeness estimation. *Sensors and Actuators B:*  
527 *Chemical*, 168, 390-394

528 Jiménez-Cuesta, M.J., Cuquerella J., Martínez-Jávega, J.M. (1981) Determination of a color  
529 index for citrus fruit degreening. In *Proc. of the International Society of Citriculture*, 2, 750-  
530 753.

531 Lado, J., Rodrigo, M.J., Zacarías, L. (2014). Maturity indicators and citrus fruit quality.  
532 *Stewart Postharvest Review*, 14, 2:2

533 Lang, C., Hübert, T. (2012) A colour ripeness indicator for apples. *Food and Bioprocess*  
534 *Technology*, 5, 3244-3249

535 Lorente, D., Aleixos, N., Gómez-Sanchis, J., Cubero, S., García-Navarrete, O.L., Blasco, J.  
536 (2012) Recent advances and applications of hyperspectral imaging for fruit and vegetable  
537 quality assessment. *Food and Bioprocess Technology*, 5, 1121-1142

538 Mendoza, F., Dejmek, P., Aguilera, J.M. (2006) Calibrated color measurements of  
539 agricultural foods using image analysis. *Postharvest Biology and Technology*, 41, 285-295

540 Molina-Martínez, J. M., Jiménez, M., Ruiz-Canales, A., Fernández-Pacheco, D. G. (2011).  
541 RaGPS: A software application for determining extraterrestrial radiation in mobile devices  
542 with GPS. *Computers and Electronics in Agriculture*, 78, 116-481

543 Montgomery, D. C. *Design and analysis of experiments*, 6th ed. Tempe: Wiley, 2005

544 Pamornnak, B., Limsiroratana, S., Chongcheawchamnan, M. (2015) Oil content  
545 determination scheme of postharvest oil palm for mobile devices. *Biosystems Engineering*,  
546 134, 8-19



547 Pongnumkul, S., Chaovalit, P. and Surasvadi, N. (2015) Applications of Smartphone-Based  
548 Sensors in Agriculture: A Systematic Review of Research. *Journal of Sensors*, 2015, Article  
549 ID 195308, 18 pages.

550 Porat, R. (2008) Degreening of citrus fruits *Tree Forest Science and Biotechnology*, 2, 71-76

551 Puder, A., Antebi, O. (2013) Cross-compiling Android applications to iOS and Windows  
552 Phone 7. *Mobile Netw. Appl.*, 18, 3–21

553 Quevedo, R., Valencia, E., Alvarado, F., Ronceros, B., Bastias, J.M. (2013) Comparison of  
554 whiteness index vs. fractal Fourier in the determination of bloom chocolate using image  
555 analysis. *Food and Bioprocess Technology*, 6, 1878-1884

556 Ramos, P.J, Prieto, F.A., Montoya, E.C., Oliveros, C.E. (2017) Automatic fruit count on  
557 coffee branches using computer vision, *Computers and Electronics in Agriculture*, 137, 9-22

558 Sabzi, S., Abbaspour-Gilandeh, Y., Javadikia, H. (2017) Machine vision system for the  
559 automatic segmentation of plants under different lighting conditions. *Biosystems*  
560 *Engineering*, 161, 157-173

561 Sengupta, S., Lee, W. S. (2014) Identification and determination of the number of immature  
562 green citrus fruit in a canopy under different ambient light conditions. *Biosystems*  
563 *Engineering*, Special Issue: Image Analysis in Agriculture, 117, 51-61

564 Vidal, A., Talens, P., Prats-Montalbán, J. M., Cubero, S., Albert, F., Blasco, J. (2013) In-  
565 Line Estimation of the Standard Colour Index of Citrus Fruits Using a Computer Vision  
566 System Developed For a Mobile Platform. *Food and Bioprocess Technology*, 6, 3412-3419